

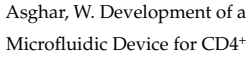
Development of a Microfluidic Device for CD4⁺ T Cell Isolation and Automated Enumeration from Whole Blood

Robert D. Fennell 1,2, Mazhar Sher 1,2 and Waseem Asghar 1,2,3,*

- Asghar-Lab, Micro and Nanotechnology in Medicine, College of Engineering and Computer Science, Boca Raton, FL 33431, USA; rfennel1@my.fau.edu (R.D.F.); msher2015@fau.edu (M.S.)
- Department of Electrical Engineering and Computer Science, Florida Atlantic University, Boca Raton, FL 33431, USA
- Department of Biological Sciences (Courtesy Appointment), Florida Atlantic University, Boca Raton, FL 33431, USA
- Correspondence: wasghar@fau.edu

Abstract: The development of point-of-care, cost-effective, and easy-to-use assays for the accurate counting of CD4⁺ T cells remains an important focus for HIV-1 disease management. The CD4⁺ T cell count provides an indication regarding the overall success of HIV-1 treatments. The CD4+ T count information is equally important for both resource-constrained regions and areas with extensive resources. Hospitals and other allied facilities may be overwhelmed by epidemics or other disasters. An assay for a physician's office or other home-based setting is becoming increasingly popular. We have developed a technology for the rapid quantification of CD4⁺ T cells. A double antibody selection process, utilizing anti-CD4 and anti-CD3 antibodies, is tested and provides a high specificity. The assay utilizes a microfluidic chip coated with the anti-CD3 antibody, having an improved antibody avidity. As a result of enhanced binding, a higher flow rate can be applied that enables an improved channel washing to reduce non-specific bindings. A wide-field optical imaging system is also developed that provides the rapid quantification of cells. The designed optical setup is portable and low-cost. An ImageJ-based program is developed for the automatic counting of CD4+ T cells. We have successfully isolated and counted CD4+ T cells with high specificity and efficiency greater than 90%.

Keywords: CD4⁺ T helper cells; microfluidic chip; microbeads; wide-field optical system; ImageJ



check for

updates

Microfluidic Device for CD4+ T Cell Isolation and Automated Enumeration from Whole Blood. Biosensors 2022, 12, 12. https:// doi.org/10.3390/bios12010012

Citation: Fennell, R.D.; Sher, M.;

Received: 12 October 2021 Accepted: 24 December 2021 Published: 28 December 2021

Publisher's Note: MDPI stays neutral with regard to jurisdictional claims in published maps and institutional affil-



Copyright: © 2021 by the authors. Licensee MDPI, Basel, Switzerland This article is an open access article distributed under the terms and conditions of the Creative Commons Attribution (CC BY) license (https:// creativecommons.org/licenses/by/ 4.0/).

1. Introduction

There is a need to develop accurate cell quantification assays to achieve early-stage disease detection, treatment, and monitoring. Various cell quantification assays have been developed, tested, and validated for a multitude of diseases over the course of time [1]. The Coulter Principle has resulted in the Coulter counters being able to measure cell size and impedance in an electrolyte solution [2,3]. The principle has been extended to interactions with light as well. As a result of these advances, several sophisticated and advanced laboratory-based devices have been tested and approved for accurate cell quantification purposes. Such devices require well-trained personnel in well-equipped laboratories. Resource-limited settings lack these facilities. Hence, there is an unmet need to develop cost-effective, easy-to-use, and rapid disease diagnostic devices at the pointof-care settings, POC. The World Health Organization (WHO) has set these guidelines for future diagnostic equipment using the acronym ASSURED, which stands for affordable, sensitive, specific, user-friendly, rapid and robust, equipment-free, and deliverable. Devices developed based on these guidelines would be equally beneficial for both resource-enabled and resource-limited countries. This lack of adequate resources also applies to physicians' offices, patients' homes, and rapidly growing telemedicine situations. Due to the need

Biosensors 2022, 12, 12 2 of 12

for speed and on-site diagnosis, the 'Sample in, Answer-out' type of assays is gaining popularity.

Early disease diagnosis is a critical factor, especially in outbreaks of infectious diseases, such as HIV (human immunodeficiency virus), Ebola, Zika, and SARS-CoV-2 [4–6]. Urgent and timely clinical decisions can help to detect and curtail the spread of infectious diseases. Sending samples and receiving their results from a clinical laboratory often takes days. Higher throughput and rapid assays are the need of the day. Currently, hospitals often create their own testing facilities to reduce the turnaround time for the same-hour diagnosis. The development of POC diagnostic tools would help to make a patient's bedside testing possible. The test results could be obtained within the least amount of time, which enables the physician to make an early clinical decision and explore further options for treatment.

POC devices are supposed to be portable, cost-effective, and environment-friendly [7–9]. It is estimated that the biosensor market will expand further in the coming years. The current developments in cellular communications, smartphone imaging systems, integrated circuit technology, along with disposable microfluidic devices, can be utilized for the future POC devices in resource-limited areas.

The CD4⁺ T count provides important information about the overall success of HIV treatment. Once HIV is diagnosed, the treatment is evaluated by the CD4⁺ T lymphocyte cell count and CD4/CD8 ratios. As the disease is treated, several assays are required. Flow cytometry is a reliable and accurate method for the quantification of CD4 cells, but it has high equipment and test costs and requires skilled resources for operation, results analyses, and maintenance. There is a dire need to develop microchip-based assays for the enumeration of CD4⁺ T cells. The main task is to isolate and quantify CD4⁺ T cells from a drop of blood. This whole process could lead to a POC assay to be used in medically resource-poor locations that cannot afford expensive diagnostic testing.

The need for microfluidic devices has been explored by a number of researchers [8,10,11]. Earlier, researchers developed a microfluidic device for the label-free CD4⁺ T cell counting of HIV-infected subjects [11]. They explored the use of a microfluidic module coated with a specific antibody for the isolation of CD4⁺ T cells and monocytes. A well-controlled fluid flow was used to separate monocytes from CD4⁺ T lymphocytes. A consistent well-controlled flow is difficult to control in a field location inside the microfluidic channel. Therefore, there is the possibility of an adverse effect on the captured CD4⁺ T lymphocytes, and, as a result, some of the cells may be forced to detach from the microchip along with the monocytes. In one other study, Moon et.al. have developed a portable microfluidic platform to count the CD4⁺ T cells of HIV-infected patients [12]. A microchip was coated with anti-CD4 antibody to capture the target CD4⁺ T cells from a fingerpick volume of whole blood. The captured cells were imaged using the lensless CCD platform. Their setup requires an automated cell counting program developed in MATLAB to identify the CD4⁺ T lymphocyte cells from monocytes.

Here, we present an alternate approach to identify CD4⁺ T cell lymphocytes from monocytes. We describe an improved microfluidic chip process that separates a sparse number of CD4⁺ T lymphocytes from whole blood samples. The developed method utilizes anti-CD4 antibody-conjugated magnetic beads to capture the CD4⁺ T cells from a drop of whole blood with high specificity. The CD4⁺ T lymphocytes are separated from monocytes with an anti-CD3 antibody-coated microchip. A washing step is then performed to get rid of the unneeded whole blood components and unattached magnetic beads from the microfluidic chip. The images of the captured CD4⁺ T cells are then recorded with the help of a custom-built wide-field optical setup. The developed wide-field optical setup helps to cover a large field of view, enabling a sufficient sample size. The images are analyzed using a computer program we developed with Image J, and the cells are counted automatically.

The developed method has several advantages over the existing microfluidic techniques. Here, the avidity improvement is caused by the utilization of an anti-CD3 antibody for coating the bottom glass substrate of the microfluidic chip along with the anti-CD4 antibody coated magnetic beads. This approach has been applied for the first time, to the

Biosensors 2022, 12, 12 3 of 12

best of our knowledge, in microfluidic-based CD4 $^+$ T cells quantification assays. Along with the enhanced antibody avidity, this approach also enabled much better CD4 $^+$ T cell isolations. Initially, we were able to isolate all the CD4 $^+$ T cells from the blood samples using the anti-CD4 coated antibody. Then, the monocytes were separated from those initially isolated CD4 $^+$ T cells using the anti-CD3 coated to the glass slide inside a microfluidic chip. We have found that the CD4 $^+$ T cells separation can be efficiently quantified using this approach with less shear stress on the cell.

2. Materials and Methods

2.1. Fabrication of the Microchip Module

The complete process list, the material source list, and a process datasheet for the microchip fabrication are presented in detail in the Supplementary Materials. The following describes the reagents, microchip design, the process design and development, the optical design and development, followed by the results obtained.

2.2. The Reagents

A complete list of materials and reagents is presented in the Supplementary Materials. Anti-CD3 antibody, UCHT1(biotin), part number ab191112 was obtained from Abcam, and it was used to coat the bottom glass substrate of the microchip. Dynabeads, part number 1145D, were obtained from ThermoFisher (Waltham, MA, USA); they were precoated with a proprietary anti-CD4 antibody.

To avoid bead clumping and unwanted adhesion to the module channel, we used ultra-pure Dulbecco's phosphate-buffered saline solution (DPBS) throughout the washing step. EDTA: ethylenediaminetetraacetic acid was used as an anticoagulant.

PMMA, a polymethylmethacrylate sheet, was utilized as the base material for making microfluidic chips. PMMA can easily be cut with a laser cutter. Various PMMA layers were joined together with the help of double-sided adhesive tape (DSA) to form a composite microfluidic chip.

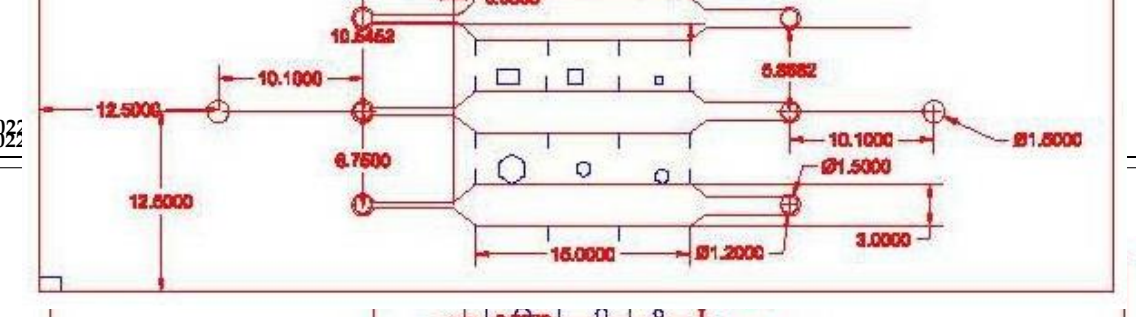
The bottom layer of a microfluidic device was chemically modified to enable antibody attachment. The in-house processing uses 3-MPS (3-Mercaptopropyl) trimethoxysilane (3-MPS, CN: 175617) and cross-linker GMBS: N- γ -Maleimidobutyryloxy succinimide ester. GMBS is a crosslinker from the amino and sulfhydryl groups. It comes as a solid and is water insoluble. Therefore, it must be mixed with DMSO or DMF [3]. We used DMSO to dissolve the GMBS so that it could be applied to the substrate.

2.3. The Microfluidic Design

A drawing of the microchip module and its photograph are shown in Figure 1. The modules were designed using AutoCAD software. The AutoCAD software was linked to a laser cutter VLS 2.30 laser cutter (VersaLaser, Scottsdale, AZ, USA). PMMA and DSA sheets were cut according to the design requirements as per previously developed method [13–16]. The dimensions of microfluidic channels were selected in such a manner that there were three microchannels in each chip for running two samples and one control.

2.4. Immobilization of Antibody to Glass Substrate

Streptavidin-coated glass slides were prepared in-house. Figure 2 presents the basic process for microchip fabrication and was previously demonstrated [7,10,17]. Briefly, a biotinylated anti-CD3 antibody was applied to the substrate. The anti-CD3, from Abcam, (Catalog No. AB191112) recognizes the CD3 antigen of the TCR/CD3 complex on mature human T cells. The antibody reacts with the epsilon chain of the CD3 complex. The developed assay utilizes the stronger avidity of anti-CD3 antibody coated on a microfluidic chip. More explanation on stronger avidity is given in the Supplement IIC.



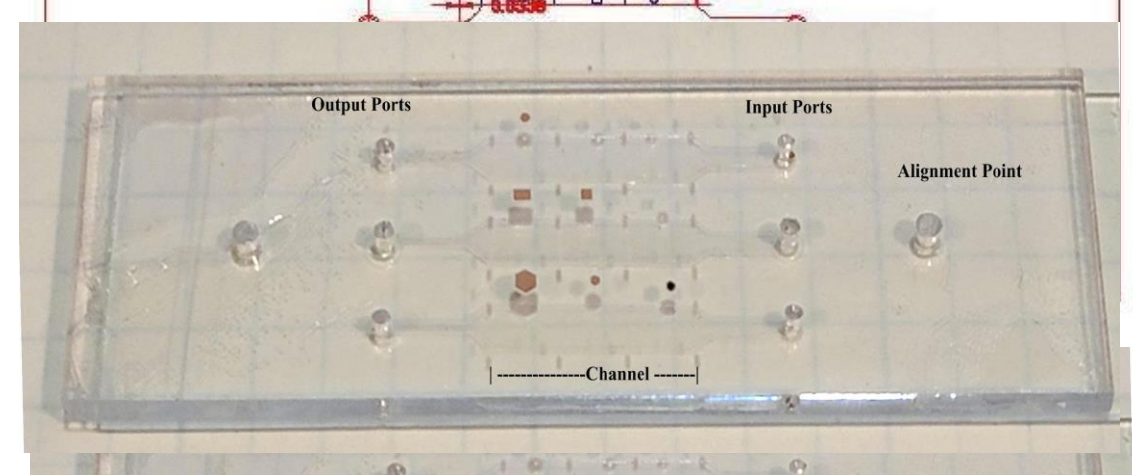
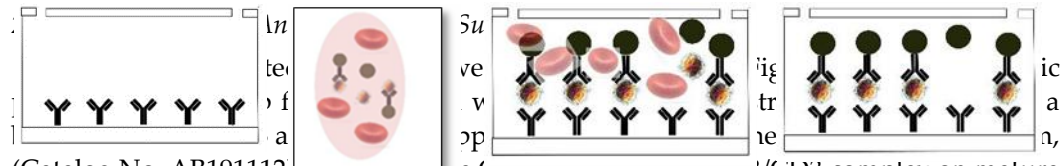


Figure 1. Microchip module with dimensions. The dimensions are the the module is the size of a typical slide, 25 × 75 mm. The channel depth is 0.076 mm.

2.4. Immobilization of Antibody to Glass Substrate

Streptavidin-coated glass slides were prepared in-house. Figure 2 presents the basic process for microchip fabrication and was previously demonstrated [7,10,17]. Briefly, a biotinylated anti-CD3 antibody was applied to the substrate. The anti-CD3, from Abcam, (Catalog No. AB191112) recognizes the CD3 antigen of the TCR/CD3 complex on mature human T cells. The antibody reacts with the epsilon chain of the CD3 complex. The developed assay utilizes the stronger avidity of anti-CD3 antibody coated on a microfluidic chip. More explanation on stronger avidity is given in the Supplement IIC.



(Catalog No. AB191112 e CD3 antigen of the CD3 complex on mature human T cells. The antibody reacts with the epsilon chain of the CD3 complex. The developed assay utilizes the stronger avidity of anti-CD3 antibody coated on a microfluidic Figure 23 Basis functionalization process (a) prepare system that the process (b) that the process (a) prepare system that the process (b) that the process (b) that the process (c) that the process (c) the process (c) that the process (c) the process (c) that the process (c) that the process (c) the process (c) that the process (c) t

Continitial processis edentian D4 patthonies (ab 2000) contraction was the standard and activation on the minimum subsection of the contraction o

was used to separate out CD4⁺ T cells along with the Dynabeads in a tube. Dynabeads Our initial process used anti-CD4 antibodies (ab 28062) on the substrate and anti-CD3 were functionalized by a custom, proprietary anti-CD4 antibody. Initially, Dynabeads were antibodies on the microspheres. We encountered difficulties in the washing process. In mixed, with the blood sample in a tube. Then, the isolation of CD4⁺ T cells was performed order to clear out the red blood cells, we need at least 50 µL/min flow rate inside microby an external magnet; the unbound entities from the blood were removed with the help fluidic channels. However, anything greater than 25 µL/min swept, out some of the white of a pipette washing. The DPBS was added to the captured beads-cell complexes, and blood cells also. We reversed the antibodies. This created an improved binding strength

beads were functionalized by a custom, proprietary anti-CD4 antibody. Initially, Dynabeads were mixed with the blood sample in a tube. Then, the isolation of CD4⁺ T cells was performed by an external magnet; the unbound entities from the blood were removed with the help of a pipette washing. The DPBS was added to the captured beads-cell complexes, and the washing step was repeated again. This second washing step was the formed to get rid of any non-desired entity. Hence, CD4+T cells and beads remained inside the tube. An HC count was then used to count the cells under an inverted microscope (Mikan Halipere T 7220) e.s.; Nikan ilappan) stadyal 1815 Angtando dasquering and togetwar ousady. Thorfoles inechen susti Ohon ver EDUh Touente diffurtientsellern hinter antialed the coule earli ETO US WAS VARE AREA OF THE CONTRACT OF THE WAS A CONTRACT OF THE CONTRACT OF TE200005c0tilkanistapathe anitooflytistic Ahitawataral sourathformathtorium CDAtal Table fore coundressed iGD4v/Excella abolated twit for the lectils following but a local from films edilusing a towals accurate do filmer clabby antailablitheit, multiplice of the other stein tight Facture logies [19], which isolatedF6iD4tnTphyriacnegtativnisebettiichic ThipseweellalsvensetheforusephasingvalD4ttiToreellsecTlin roumbethef galizatell challen istoliated lewithorth fulled potry lover to be additively poor first many discount of the content of the conten alternalatest connocritically wavised about 15 is interesting of Microsoft Stephanological for the state of the contraction of isoda test CDAthTalFhaonesatint Cellebriage TOECE; BlovRent Llatroristodies at validates oc Apells a) ovitlo 2 the object ledecharmed in in the images of the idic device to verify the process. As an additional test to nondymawhits callide Difigations. Whe Blund and Innorman antrounterstain who want vcitts a Fhilorescenth Cell Lanzgerol Z. Pfg Bie-Rad Leaby satories "Vlerchiletel Claw J. Saltenitth 20 kr Objective length and implicit structures of the microfluidic chip channel.

The Bywale and walk the ella were injected interted in every injection of the anti-CP3. The bound of the property of the property of the ella were the entire that the entire the entire that the ella were the entire that th

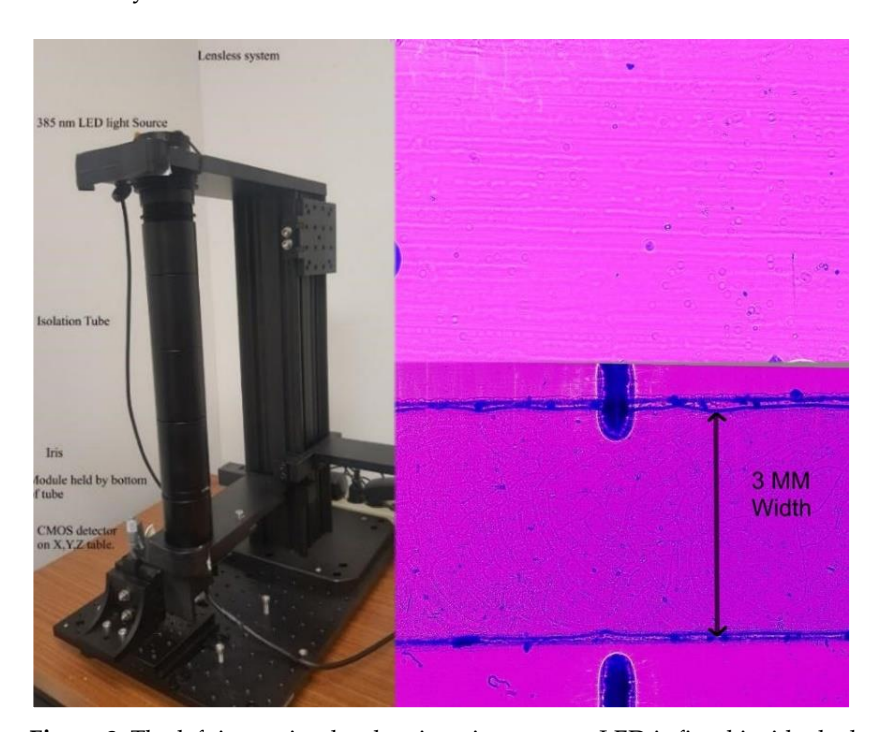


Figure 3. The left image is a lendless imaging system. LED's fitted insket had uning connected to leave the bound of the principal state. The light passes through the pinhole and shadow patterns of beads/cells are produced on EMOS sensor mounted on the base part. The chip containing captured cells and beads is placed on EMOS sensor before taking the image. The upper containing captured cells and beads is placed on EMOS sensor before taking the image. The upper right lensless image was enlarged and shows beads and cells in a microfluidic chip module. The bottom right image shows the typical width of field, which is that of the imaging device.

DPBS was used to wash the channels that reduced the clumping of beads and cells. The channel washing was performed at a high flow rate of 50 μ L/minute for 8 min. There were only a few beads not attached to CD4⁺ T cells that were left in the channel.

2.5. Measurement of Capture Efficiency

As previously mentioned, the cell isolation process used the double selection method with anti-CD4 antibody-coated Dynabeads and an anti-CD3 antibody immobilized to the glass slide. The images of the captured cells were taken using the microscope and are called the microscope count, MC. The image areas, microchip channel volume, and

Biosensors 2022, 12, 12 6 of 12

dilution amount are taken into account. Multiple images are necessary because the inverted microscope (Nikon Eclipse TE2000-S) trades off magnification for coverage area, and the CD4⁺ T count can be low per unit area. A wide area imaging technique was developed in earlier work [20] to compensate for this, and the design is described in Section 3 D. Capture efficiency was then the module microscope count (MC) divided by HC, the hemocytometer count. The module count, MC, was done by stitching together 8 photographs down a channel and then counting the CD4⁺ T cells. In both cases, at this magnification, resolution, and narrow field of view, the low number of cells visible per image requires several different pictures to get a sufficient sample. This is also true for a hemocytometer, HC, where several photos were taken over several sectors. The images were then reviewed and CD4⁺ T cells were identified and counted per unit volume.

MC: count on inverted microscope (Nikon Eclipse TE2000-S) of the microchip module. HC: count on inverted microscope (Nikon Eclipse TE2000-S) of the hemocytometer, Dynabeads process.

Efficiency =
$$MC/HC\%$$
 (1)

2.6. Measurement of Specificity

To verify our process separation of CD4 $^+$ T cells, a cell permeant counterstain was used, NucBlue, (Hoechst 33342), that emits blue fluorescent light at 460 nm when bound to DNA and excited by UV light. A Fluorescent Cell Imager (ZOE, Bio-Rad Laboratories, Hercules, CA, USA) with $20\times$ objective lens was used. Brightfield (BF) and fluorescent images (FC) were created, stored, and merged, as shown in Figure S2 of the Supplement. An ImageJ program was then used to count cells and compare the BF and FC count. Visual confirmation was done with the merged view. Specificity was then the FC divided by BF.

Specificity =
$$FC/BF\%$$
 (2)

2.7. Development of a Lensless System to Enable Wide-Field-Imaging

In the development of a lensless imaging system, the key design issue is to generate a near monochromatic light source to ensure a parallel source without scattering. The module needs to be as close as possible to the CCD imaging device. An experimental lab-quality device was built as shown in Figure 3. It has the advantage of an X, Y, Z incremental movement of the microchip module. Multiple channels can easily be observed and brought into view. A portable lensless device is shown in Figure 3 that is suitable for a single channel micromodule. A lensless system is capable of magnification due to the projection of the image over a distance, and that diffraction widens the image with airy disks. The images are not focused due to diffraction and the non-coherence of the wave. Computer enhancement software was used that performs reverse diffraction [21]. The diffraction patterns recorded by the CMOS image sensor were reverse diffracted using the angular spectrum method (ASM). The program takes into account the diffraction distance, wavelength of light, and pixel size. For the lensless case, the resolution was improved from 23 lines per mm to 29 Lp/mm [20]. The imaging setup had a field of view of 6.14 mm \times 4.604 mm and had a small pixel size (1.25 µm) that enabled digital magnification of small objects, such as small microbeads or cells.

2.8. Process for Imaging and Counting Cells

The CD4 $^+$ T cells isolated from a blood sample can be counted manually. A visual examination is needed for the identification of CD4 $^+$ T cells from unattached beads and debris. If the sample can be sufficiently purified to mainly CD4 $^+$ T cells and attached Dynabeads, then automatic counting based on the area can be employed to distinguish cells from one another. The ImageJ [22,23] program was customized to automatically count cells that were photographed on an inverted microscope (Nikon Eclipse TE2000-S) at $10\times$. The Supplement provides details of the process of using ImageJ for various objects and conditions. The parameters were also optimized for images from the Fluorescent Cell

Biosensors 2022, 12, 12 7 of 12

Imager (ZOE, Bio-Rad Laboratories, Hercules, CA, USA) with $20\times$ objective lens and for the images from lensless systems. The parameters are based on the type of object being imaged. We were able to distinguish CD4⁺ T cells and the beads that were not attached to cells. Dapi or NucBlue stains were used for fluorescence verification.

The Supplement I B. titled "Process for imaging and Counting Cells in ImageJ" and Supplementary Table S1 show the basic ImageJ process parameters for counting the cells.

3. Results

3.1. Capture of CD4⁺ T Cells and Monocytes Using Dynabeads

Dynabeads functionalized with anti-human CD4 antibody (ThermoFisher, part number 11145D) [24] were utilized for the positive isolation of CD4⁺ T cells from whole blood samples. EDTA was added to the fresh blood as an anticoagulant. Moreover, ultrapure DPBS was used for washing purposes. The CD4 glycoprotein is expressed on two types of cells, i.e., CD4⁺ T lymphocytes and CD4⁺ monocytes. However, CD4⁺ T lymphocytes also express CD3 glycoprotein, whereas CD4⁺ monocytes do not express this CD3 antigen. Therefore, we used this biomarker to isolate the pure population of CD4⁺ T lymphocytes by binding them to the substrate and washing out the monocytes.

3.2. Microfluidic Device Process Verification

The CD4⁺ T cell isolation process was first verified by the standard method using an inverted microscope (Nikon Eclipse TE2000-S), a hemocytometer, and a Fluorescent Cell Imager (ZOE, Bio-Rad Laboratories, Hercules, CA, USA) microscope. Figure 4 presents the image of the cells obtained with the Fluorescent Cell Imager (ZOE, Bio-Rad Laboratories, Hercules, CA, USA). The lensless system that was developed could then be accurately utilized to the count the CD4⁺ T cells from the blood samples. The gold standard used biosensors 2022, 12, × FOR PEER REVIEW comparison was the standard Dynabeads magnetic separation with a hemocytometer. Count (HC) on an inverted microscope (Nikon Eclipse TE2000-S). Figure 5 portrays the

Dynabeads and Dynabeads with attached CD4⁺ T cells on a section of the hemocytometer.

10 um

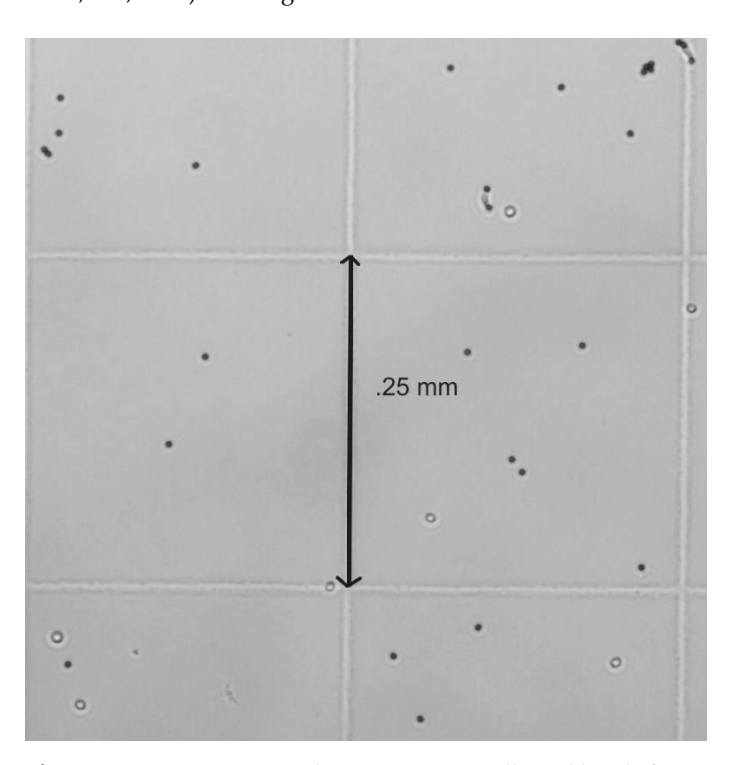
rfigure 4.4 EAN of the Property of the Propert



8 of 12

Figure 4. Enlarged merged image from Fluorescent Cell Imager (ZOE, Bio-Rad Laboratories, Hercules, CA, USA) showing beads and white cells.

10 um



rightes. Hemocytometershowing GD4* T cells and beads from standard Dynabeads process. Note that the normal Dynabeads process does not remove unattached beads since the magnetic force cannot distinguish the difference. Visual identification is required for area calculations.

3.3. Process Veriffication Results with Blood Samples

The Continental Blood Bank, Ibrated Ibrally in Fort I Lautherdale, HI, was the source of several different whole blood samples from which we were able to successfully isolate, itlentify and count the CD4+T cells using a microdip module. A wide field optical satup and an automatic counting pretable over used to findinal ideal counting the field optical satup and an automatic counting pretable over used to findinal ideal counting the field of th

Table 1. Process efficiency of the micromodule based on inverted microscope (Nikon Eclipse TE2000-S) measurements.

Sample	HC Hemocytometer Count	MC Cell Count	Efficiency %
Sample 1 Blood	214	178	86
Sample 2 Blood	380	392	103
Sample 3 Blood (Processed with EasySep kit)	1592	1680	106
Average			98.3 ± 10.8

The microfluidic device process was proven to be effective. Table 1 portrays the efficiency of the process when comparing the microchip-based CD4⁺ T cell count to the hemocytometer count when using the Nikon as the imaging device. Multiple images are necessary for both the hemocytometer and the microchip module to ensure a sufficient

Biosensors 2022, 12, 12 9 of 12

sample. This is a standard procedure for the hemocytometer, and the cells were visually identified and averaged. We were able to take a string of images (eight consecutive images) down the center of the microchip module and form a unified image. Given a known volume and area of the module, the concentration could be calculated. The small field of view offered by a regular optical microscope demonstrated the need to create a widefield imaging system. We develop these simplified systems as presented in the wide-field imaging section.

Table 2 shows the results of three different blood samples and their specificity. The same image was taken as a fluorescent image and then a bright-field image. The Fluorescent Cell Imager (ZOE, Bio-Rad Laboratories, Hercules, CA, USA) merged view shows a good correlation between the bright field and the blue field. NucBlue was used as the UV dye because it works with both alive and dead cells. It is anticipated that the final field process will be dealing primarily with live cells since the assay time will be short.

Table 2. Fluorescent Cell Imager (ZOE, Bio-Rad Laboratories, Hercules, CA, USA) used for specificity	y
measurement. Cells/image.	

Sample	FC Blue Count	BF Bright Field	Specificity %
Sample 4 Blood	345	414	83
Sample 5 Blood	380	449	85
Sample 6 Blood (Processed with EasySep kit)	311	311	100
Average			89.3 ± 9.3

The microchip process has been proven for cell isolation efficiency (98.3 \pm 10.8%) and specificity (89.3 \pm 9.3%), as shown in Tables 1 and 2, respectively. The next step is to show the results when using a lensless or wide-field lens system. The cell isolation efficiency was 88.5 \pm 9.2%, as shown in Table 3. The specificity was already proven with the fluorescent imaging system.

Table 3. Lensless cell count efficiency using a lensless or lens optical system.

Sample Blood	Hemocytometer Count (HC)	Lensless Cell Count	Percentage Efficiency
Sample 7 Blood	380	311	82
Sample 8 Blood	480	457	95
Average			88.5 ± 9.2

3.4. Validation of Module Process and Counting Using Wide-Field Imaging

The microfluidic chip modules integrated with a lensless imaging system were designed to have a wide field of view so that the large surface area of the chip can be imaged rapidly. In CD4⁺ T cell isolation experiments, the number of cells to be counted per unit area is small. It is necessary to have either multiple images or a wide-area imaging system to capture a sufficient sample within the channel of the module.

Our previous work [20] has shown that wide-field lensless and custom-designed lens systems are possible. A low-cost lensless system is also described in that paper. For this work, we used the optical systems we had previously developed. A lensless system has a wide field of view, conforming to the size of the imaging field-of-view, in this case, 6.14×4.6 mm, as shown in Figure 3. The resolution is limited by the size of the pixel (1.25 um in this case) and the image area by the size of the array, 18 Megapixels. Figure 3 also portrays an enlarged section of the microchip module and shows the beads and CD4 $^+$

Biosensors 2022, 12, 12 10 of 12

T cells. Table 3 shows that the CD4⁺ T cell isolation efficiency was at 89 \pm 9.19 for the lensless system.

3.5. Conclusion and Discussion

A microfluidic chip-based assay has been developed that can sort out CD4⁺ T lymphocytes and count them using a microfluidic device, rather than magnetic separation, with excellent specificity and efficiency. The developed process was proven to be successful and provides $89.3 \pm 9.3\%$ capture specificity and $98.3 \pm 10.8\%$ capture efficiency inside microfluidic channels. The processes have been simplified such that a portable microchip design is possible for point-of-care use.

A wide-field optical system was explored, and its properties and limitations were examined. Lensless equipment was designed, built, and tested to complement the microchip design. This imaging system allows a larger sample area to enable the accurate counting and recognition of biological samples that normally have a low count per unit volume but at a lower cost per assay. The ImageJ-based algorithm was structured and used to automatically count cells. In the future, artificial intelligence could be used to better identify different types of cells.

Simple systems, such as lensless or wide-field lens systems, can be used at the point-of-care locations. This microfluidic device will enable wide-field optical systems to capture a sufficient area to count a low number of cell assays. Overall, the developed method is cost-effective, easy to use, and rapid, and can be used for counting CD4⁺ T cells at the point-of-care settings.

Supplementary Materials: The following supporting information can be downloaded at: https://www.mdpi.com/article/10.3390/bios12010012/s1, Figure S1. Process Flow Data Sheet. Figure S2. From left to right The Bright field Image on Fluorescent Cell Imager (ZOE, Bio-Rad Laboratories, Hercules, CA, USA). The Blue Field Image and The Merge Image, used to calculate Specification. Note the large im-age but small size of cells. Table S1. Key ImageJ parameters for analyze

Author Contributions: Conceptualization, W.A., R.D.F. and M.S.; methodology, W.A., R.D.F. and M.S.; software, R.D.F.; validation, R.D.F., M.S. and W.A.; formal analysis, W.A., R.D.F. and M.S.; investigation, R.D.F., M.S. and W.A.; resources, W.A.; data curation, R.D.F. and M.S.; writing—original draft preparation R.D.F., M.S. and W.A.; writing—review and editing, R.D.F., M.S. and W.A.; visualization, R.D.F.; supervision, W.A. and M.S.; project administration, W.A. and M.S.; funding acquisition, W.A. All authors have read and agreed to the published version of the manuscript.

Funding: This research was funded by National Institute of Health (NIH) grant number R56AI138659, NSF CAREER Award 1942487, and Humanity in Science Award.

Institutional Review Board Statement: Not applicable.

Informed Consent Statement: Not applicable.

Data Availability Statement: Not applicable.

Acknowledgments: We are thankful to William Rhodes for help on near and far-field theory, Oge Marques for computer analysis of images, Benjamin Coleman for technical discussions, and Charles Perry Wienthal for allowing us to use CEECS lab facilities to fabricate various 3D components. We also thank Diya Jain (Pine Crest School) for helping in proofreading the manuscript.

Conflicts of Interest: The authors declare no conflict of interest.

Biosensors **2022**, 12, 12

Abbreviations

Antibody (Clone 13B8.2, CN: COIM0704) was purchased from Fisher Scientific (Fair Lawn, NJ, USA)

APTES slide APTES, 3-Aminopropyl Trimethoxysilane treated slide

ASSURED Affordable, sensitive, specific, user-friendly, rapid and robust, equipment-free,

and deliverable

lyophilized bovine serum albumin (BSA, CN a2153). A small stable protein of 607 amino

acids, it is used as a blocker to help antibodies find antigens by binding to non-specific

oinding sites

Dimethyl sulfoxide is polar organic solvent that is miscible with water. We mixed the GMBS

DMSO with DMSO so that it can be further cut and soluble in water. We can then apply to our

substrate. So that GMBS can adhere to the substrates, we have a double bond to the surface

DPBS D phosphate-buffered saline solution

DSA Double sided adhesive tape. Forms the channel and binds the top and bottom layer in the

micro module

EDTA Ethylenediaminetetraacetic acid; prevents the coagulation of blood cells by absorbing mental

ions to prevent binding of beads and blood

N-γ-Maleimidobutyryloxy succinimide ester; this is a chemical that is a cross linker from

amino and sulfhydryl groups. It comes as a solid and is water insoluble. Therefore, must be

mixed with DMSO or DMF [3]. We use DMSO

HC Hemocytometer count

HIV Human immunodeficiency virus

Maleimide Activated Neutravidin This version can bond directly without using GMBS to cross link to slide

MC Microscope count

MPS (3-Mercaptopropyl) trimethoxysilane (3-MPS, CN: 175617), b. This compound is an adhesive;

it has four hydrogen acceptor molecules and one donator

It is the first layer to adhere to a glass slide that has donor atoms

Neutravidin protein This protein is used to attach to the GMBS and the anti-CD4 antibody. $Ka = 10^{15} M^{-1}$ NucBlue This stain is best for live and dead cells. It is from Invitrogen and similar to DAPI PMMA Polymethymetacrylate sheet. It is an acrylic sheet that can be easily cut with a laser cutter

POC Point-of-care

WHO World Health Organization

Other items used were: anti-CD4 beads, absolute alcohol: ethanol 200 proof, OH-, and glass slides

References

BSA

GMBS

1. Kosack, C.S.; Page, A.-L.; Klatser, P.R. A guide to aid the selection of diagnostic tests. *Bull. World Health Organ.* **2017**, 95, 639. [CrossRef] [PubMed]

- 2. Hassan, U.; Reddy, B., Jr.; Damhorst, G.; Sonoiki, O.; Ghonge, T.; Yang, C.; Bashir, R. A microfluidic biochip for complete blood cell counts at the point-of-care. *Technology* **2015**, *3*, 201–213. [CrossRef] [PubMed]
- 3. Hassan, U.; Watkins, N.; Edwards, C.; Bashir, R. Flow metering characterization within an electrical cell counting microfluidic device. *Lab Chip* **2014**, *14*, 1469–1476. [CrossRef] [PubMed]
- 4. Sher, M.; Coleman, B.; Caputi, M.; Asghar, W. Development of a Point-of-Care Assay for HIV-1 Viral Load Using Higher Refractive Index Antibody-Coated Microbeads. *Sensors* **2021**, *21*, 1819. [CrossRef] [PubMed]
- 5. Sher, M.; Faheem, A.; Asghar, W.; Cinti, S. Nano-Engineered Screen-Printed Electrodes: A dynamic tool for detection of Viruses. *TrAC Trends Anal. Chem.* **2021**, 143, 116374. [CrossRef] [PubMed]
- 6. Kabir, M.A.; Zilouchian, H.; Sher, M.; Asghar, W. Development of a flow-free automated colorimetric detection assay integrated with smartphone for Zika NS1. *Diagnostics* **2020**, *10*, 42. [CrossRef] [PubMed]
- 7. Shafiee, H.; Asghar, W.; Inci, F.; Yuksekkaya, M.; Jahangir, M.; Zhang, M.H.; Durmus, N.G.; Gurkan, U.A.; Kuritzkes, D.R.; Demirci, U. Paper and flexible substrates as materials for biosensing platforms to detect multiple biotargets. *Sci. Rep.* **2015**, *5*, 8719. [CrossRef] [PubMed]
- 8. Wasserberg, D.; Zhang, X.; Breukers, C.; Connell, B.J.; Baeten, E.; van den Blink, D.; Benet, E.S.; Bloem, A.C.; Nijhuis, M.; Wensing, A.M.J.; et al. All-printed cell counting chambers with on-chip sample preparation for point-of-care CD4 counting. *Biosens. Bioelectron.* **2018**, 117, 659–668. [CrossRef] [PubMed]
- 9. Sher, M.; Zhuang, R.; Demirci, U.; Asghar, W. Paper-based analytical devices for clinical diagnosis: Recent advances in the fabrication techniques and sensing mechanisms. *Expert Rev. Mol. Diagn.* **2017**, *17*, 351–366. [CrossRef] [PubMed]
- 10. Asghar, W.; Yuksekkaya, M.; Shafiee, H.; Zhang, M.; Ozen, M.O.; Inci, F.; Kocakulak, M.; Demirci, U. Engineering long shelf life multi-layer biologically active surfaces on microfluidic devices for point of care applications. *Sci. Rep.* **2016**, *6*, 21163. [CrossRef] [PubMed]

Biosensors 2022, 12, 12 12 of 12

11. Cheng, X.; Irimia, D.; Dixon, M.; Sekine, K.; Demirci, U.; Zamir, L.; Tompkins, R.G.; Rodriguez, W.; Toner, M. A microfluidic device for practical label-free CD4⁺ T cell counting of HIV-infected subjects. *Lab Chip* **2007**, *7*, 170–178. [CrossRef] [PubMed]

- 12. Moon, S.; Gurkan, U.A.; Blander, J.; Fawzi, W.W.; Aboud, S.; Mugusi, F.; Kuritzkes, D.R.; Demirci, U. Enumeration of CD4⁺ T-cells using a portable microchip count platform in Tanzanian HIV-infected patients. *PLoS ONE* **2011**, *6*, e21409. [CrossRef] [PubMed]
- 13. Asghar, W.; Sher, M.; Khan, N.S.; Vyas, J.M.; Demirci, U. Microfluidic chip for detection of fungal infections. *ACS Omega* **2019**, *4*, 7474–7481. [CrossRef] [PubMed]
- 14. Ilyas, S.; Sher, M.; Du, E.; Asghar, W. Smartphone-Based sickle cell disease detection and monitoring for point-of-care settings. *Biosens. Bioelectron.* **2020**, *165*, 112417. [CrossRef] [PubMed]
- 15. Rappa, K.; Samargia, J.; Sher, M.; Pino, J.S.; Rodriguez, H.F.; Asghar, W. Quantitative analysis of sperm rheotaxis using a microfluidic device. *Microfluid. Nanofluid.* **2018**, 22, 100. [CrossRef]
- 16. Coarsey, C.; Coleman, B.; Kabir, M.A.; Sher, M.; Asghar, W. Development of a flow-free magnetic actuation platform for an automated microfluidic ELISA. *RSC Adv.* **2019**, *9*, 8159–8168. [CrossRef] [PubMed]
- 17. Sher, M.; Asghar, W. Development of a multiplex fully automated assay for rapid quantification of CD4⁺ T cells from whole blood. *Biosens. Bioelectron.* **2019**, *142*, 111490. [CrossRef] [PubMed]
- 18. Counting-Cells-Using-A-Hemocytometer. Available online: https://docs.abcam.com/pdf/protocols/counting-cells-using-a-hemocytometer.pdf (accessed on 23 December 2021).
- 19. EasySep Cell Separation. Available online: https://www.stemcell.com/products/brands/easysep-cell-separation.html (accessed on 23 December 2021).
- 20. Fennell, R.D.; Sher, M.; Asghar, W. Design, development, and performance comparison of wide field lensless and lens-based optical systems for point-of-care biological applications. *Opt. Lasers Eng.* **2021**, *137*, 106326. [CrossRef] [PubMed]
- 21. Stork, D.G.; Ozcan, A.; Gill, P.R. Imaging Without Lenses: New imaging systems, microscopes, and sensors rely on computation, rather than traditional lenses, to produce a digital image. *Am. Sci.* **2018**, *106*, 28–34. [CrossRef]
- 22. Abramoff, M.D.; Magalhães, P.J.; Ram, S.J. Image processing with ImageJ. Biophotonics Int. 2004, 11, 36–42.
- 23. Imagej. Available online: https://imagej.nih.gov/ij/download.html (accessed on 23 December 2021).
- Dynabeads_Cell_Separation_Guide. Available online: https://assets.fishersci.com/TFS-Assets/LSG/brochures/Dynabeads_cell_separation_guide.pdf (accessed on 23 December 2021).